

# REPORT 1111

## AN ANALYSIS OF LAMINAR FREE-CONVECTION FLOW AND HEAT TRANSFER ABOUT A FLAT PLATE PARALLEL TO THE DIRECTION OF THE GENERATING BODY FORCE<sup>1</sup>

By SIMON OSTRACH

### SUMMARY

*The free-convection flow and heat transfer (generated by a body force) about a flat plate parallel to the direction of the body force are formally analyzed and the type of flow is found to be dependent on the Grashof number alone. For large Grashof numbers (which are of interest in aeronautics), the flow is of the boundary-layer type and the problem is reduced in a formal manner, which is analogous to Prandtl's forced-flow boundary-layer theory, to the simultaneous solution of two ordinary differential equations subject to the proper boundary conditions.*

*Velocity and temperature distributions for Prandtl numbers of 0.01, 0.72, 0.733, 1, 2, 10, 100, and 1000 are computed, and it is shown that velocities and Nusselt numbers of the order of magnitude of those encountered in forced-convection flows may be obtained in free-convection flows. The theoretical and experimental velocity and temperature distributions are in good agreement.*

*A flow and a heat-transfer parameter, from which the important physical quantities such as shear stress and heat-transfer rate can be computed, are derived as functions of Prandtl number alone. Comparison of theoretically computed values of the heat-transfer parameter with values obtained from an approximate calculation and experiments yielded good agreement over a large range of Prandtl number. Agreement between the theoretical values and those obtained from a frequently used semiempirical heat-transfer law was good only in restricted Prandtl number ranges (depending on an arbitrary constant).*

### INTRODUCTION

Two important types of fluid flow problems involving heat transfer are those of forced and those of free convection. By forced-convection flow is meant flows maintained mechanically as, for example, by a pressure drop or an agitator. Free-convection flow, on the other hand, results from the action of body forces on the fluid, that is, forces which are proportional to the mass or the density of the fluid. The flow is generally produced in the following manner: Consider, for example, a fixed object (such as a plate) in a quiescent fluid subject to a body force. When the plate is at the same temperature as the surrounding fluid, the body forces acting on the fluid are in equilibrium with the hydrostatic pressure and no flow ensues in the steady state. If a temperature gradient normal to the body force is imposed by heating (or cooling) the plate, there will exist a defect (or excess) of

body force because of the decreased (or increased) density, with the fluid closer to the plate having the greater defect (or excess) than that away from the plate. This unbalance of the forces causes the fluid to be accelerated with the particles nearer the plate moving more rapidly than those farther from the plate. Free-convection flow has usually been considered to be generated in a gravitational field where the previously mentioned defect or excess of body force was the Archimedian (buoyancy) force. However, since centrifugal forces are also proportional to the fluid density, free-convection flows can also be set up by the action of such forces. (See ref. 1 for a more explicit discussion of the development of free-convection flows by centrifugal forces.)

Free-convection flows produced by centrifugal forces are now of practical importance in aeronautics because many aircraft propulsion systems contain components (such as gas turbines and helicopter ram jets) which rotate at high speeds and in which heat is being transferred. The method of free-convection cooling of gas-turbine rotor blades where the centrifugal forces create a free-convection flow of the coolant in the blade passages is an example of a practical application of the free-convection phenomenon in aeronautics. Also, free-convection flow due to centrifugal force is superimposed on the flow through helicopter ram jets and on the flow of cooling air in hollow rotor blades of air-cooled turbines and, under proper conditions, can appreciably influence the resultant flow and heat transfer.

As a simplification of the many free-convection problems which are now of some consequence in aeronautics, consideration is here given to the special case of free-convection flow about a flat plate parallel to the direction of the generating body force. The experimental and theoretical considerations of Schmidt and Beckmann (ref. 2) concerning the free-convection flow of air subject to the gravitational force about a vertical flat plate constitute the most complete treatment of this subject up to the present time. Eckert (ref. 1) as well as others has further verified and extended the experimental results of Schmidt and Beckmann, and Schuh (ref. 3) has extended the numerical calculations by computing the velocity and temperature distributions for several Prandtl numbers different from that for air. However, all the theoretical work in these references is based on the incompressible equations in which the density (or temperature) variation is introduced in the buoyancy term alone.

<sup>1</sup> Supersedes NACA TN 2635, "An Analysis of Laminar Free-Convection Flow and Heat Transfer about a Flat Plate Parallel to the Direction of the Generating Body Force" by Simon Ostrach, 1952.

Various terms are omitted from the equations at the start on the basis of either intuitive arguments or no arguments at all. Although a theoretical development made in such a manner led to good final results, the significance of all the important factors associated with the free-convection flow phenomenon is not obtained from such an analysis.

The problem of free-convection flow as produced by a body force about a flat plate in the direction of the body force was studied at the NACA Lewis laboratory during 1951 and is treated in a formal and more general manner herein. The method used is somewhat similar to that used in reference 4 wherein consideration was given to the free-convection flow at high Grashof numbers in a horizontal cylinder which had a variable surface-temperature distribution. The application of this method to the present problem leads to a development which is analogous to Prandtl's treatment of high Reynolds number forced-convection flows. Although the final equations obtained by this method are the same as those of Schmidt and Beckmann, this more general approach not only clearly demonstrates the significance of all the important parameters and assumptions and hence leads to a better understanding of this type of flow but also indicates the quantitative limitations of the theory. In addition, the numerical solutions of references 2 and 3 are herein extended to cover a more complete range of parameters. The new calculations yield information on the free-convection flow for Prandtl numbers corresponding to those of liquid metals, gases, liquids, and very viscous fluids.

#### ANALYSIS

##### STATEMENT OF PROBLEM AND BASIC EQUATIONS

The steady-state equations expressing the conservation of mass, momentum, and energy for a compressible, viscous, and heat-conducting fluid subject to a body force together with an equation of state govern the flow and associated temperature distribution about the plate. These equations in Cartesian tensor notation are (see ref. 5), respectively,

$$\frac{\partial}{\partial X_j} (\rho U_j) = 0 \quad (1)$$

$$\rho U_j \frac{\partial U_i}{\partial X_j} = \rho f_i + \frac{\partial}{\partial X_j} \left[ \mu \left( \frac{\partial U_i}{\partial X_j} + \frac{\partial U_j}{\partial X_i} \right) \right] - \frac{2}{3} \frac{\partial}{\partial X_i} \left( \mu \frac{\partial U_j}{\partial X_j} \right) - \frac{\partial P}{\partial X_i} \quad (2)$$

$$\rho c_p U_j \frac{\partial T}{\partial X_j} = U_j \frac{\partial P}{\partial X_j} + \frac{\partial}{\partial X_j} \left( k \frac{\partial T}{\partial X_j} \right) + \mu \left[ \frac{\partial U_i}{\partial X_j} \left( \frac{\partial U_i}{\partial X_j} + \frac{\partial U_j}{\partial X_i} \right) - \frac{2}{3} \left( \frac{\partial U_j}{\partial X_j} \right)^2 \right] \quad (3)$$

$$\rho = \rho(P, T) \quad (4)$$

(A complete list of the symbols used herein is given in appendix A.) For the two-dimensional case, equations (1) to (4) represent a system of five equations in the five dependent variables  $U_1$ ,  $U_2$ ,  $\rho$ ,  $P$ , and  $T$ . For later use, equation (4) can be written

$$d\rho = \rho(K dP - \beta dT) \quad (4a)$$

where  $K$  and  $\beta$  are the coefficients of isothermal compressibility and volumetric expansion, respectively (see ref. 6). In addition to a general state equation, such as is given in equations (4) or (4a), it will be convenient at times in the discussion to refer to some specific state equation. To this end, the equation of state for an ideal gas

$$P = \rho RT \quad (4b)$$

will be used.

Particular consideration is here given to the two-dimensional free-convection flow about a semi-infinite vertical flat plate. The  $X_1$ -axis of the coordinate system is taken along the plate and the  $X_2$ -axis, normal to it. No distinction is made as to the specific type of body force acting, for example, gravitational or centrifugal, but the force is assumed to be acting in the vertical direction only (that is, parallel to the plate). Centrifugal and Coriolis forces which are connected with flows on curved paths and with rotating systems generally vary with position and velocity. However, in order not to make the analysis unduly complicated, the body force is taken to be constant.

In order to define the problem clearly, a choice must still be made of the position of the origin of the coordinate system. Before making a definite decision on this point, note that for constant plate temperatures there are four permutations of the body-force direction (either upward or downward) and the plate thermal condition (either heated or cooled) which will lead to free-convection flows. Once the position of the edge of the plate, which is also to be the origin of the coordinate system, is decided, there are two combinations of the body-force direction and plate thermal condition that will yield flows which proceed away from the edge. It is this type of flow that is amenable to the type of analysis to be made here. This point will be more fully discussed subsequently. If the edge of the plate (recall that a semi-infinite plate has but one edge) is taken at the bottom of the plate (that is, the plate extends to  $+\infty$  in the  $X_1$ -direction), the two combinations leading to flows in the proper direction (upward in this case) are, respectively, the body force acting downward with a heated plate and the body force acting upward with a cooled plate. The equations developed for one of the cases reduce directly to those for the other. The remaining two permutations, namely, the body force acting downward with a cooled plate and the body force acting upward with a heated plate, would yield flows which proceed downward or toward the edge of the plate if this edge were taken at the bottom of the plate. This type of flow would violate a physical condition of the problem which states that the flow starts at the plate edge. The latter combinations hence will not be considered further.

Because the two acceptable configurations can be reduced essentially to one, for the development to be given here, the origin of the coordinate system will be taken at the bottom of a heated plate, with the body force acting downward. The assumption is now made that the viscosity and thermal-conductivity coefficients are functions of the temperature alone and obey the following laws:

$$\left. \begin{aligned} \mu &= \mu_\infty \left( \frac{T}{T_\infty} \right)^m \\ k &= k_\infty \left( \frac{T}{T_\infty} \right)^n \end{aligned} \right\} \quad (5)$$

The choice of the body-force direction together with equations (5) alters equations (2) and (3) so that they become

$$\rho U_j \frac{\partial U_i}{\partial X_j} = -\rho(-f_i) + \frac{\mu_\infty}{T_\infty^m} \frac{\partial}{\partial X_j} \left[ T^m \left( \frac{\partial U_i}{\partial X_j} + \frac{\partial U_j}{\partial X_i} \right) \right] - \frac{2}{3} \frac{\mu_\infty}{T_\infty^m} \frac{\partial}{\partial X_i} \left( T^m \frac{\partial U_j}{\partial X_j} \right) - \frac{\partial P}{\partial X_i} \quad (6)$$

$$\rho c_p U_j \frac{\partial T}{\partial X_j} = U_j \frac{\partial P}{\partial X_j} + \frac{k_\infty}{T_\infty^n} \frac{\partial}{\partial X_j} \left( T^n \frac{\partial T}{\partial X_j} \right) + \frac{\mu_\infty}{T_\infty^m} T^m \left[ \frac{\partial U_i}{\partial X_j} \left( \frac{\partial U_i}{\partial X_j} + \frac{\partial U_j}{\partial X_i} \right) - \frac{2}{3} \left( \frac{\partial U_j}{\partial X_j} \right)^2 \right] \quad (7)$$

Note that the only nonzero component of the body force is the  $X_1$ -component.

BOUNDARY CONDITIONS

The boundary conditions associated with the given problem are that:

(a) The fluid must adhere to the plate (the no-slip condition of viscous flows) and the plate must be a streamline, or mathematically,

$$U_1(X_1, 0) = U_2(X_1, 0) = 0 \quad (8)$$

(b) The temperature of the fluid at the plate must be equal to the plate temperature, that is,

$$T(X_1, 0) = T_0 \quad (9)$$

(c) The velocity  $U_1$  at large distances from the plate must be undisturbed, or

$$U_1(X_1, \infty) = 0 \quad (10)$$

(d) The temperature at large distances from the plate must be equal to the undisturbed fluid temperature, or

$$T(X_1, \infty) = T_\infty \quad (11)$$

SIMPLIFICATION OF EQUATIONS

Let a small quantity  $\epsilon$  now be defined as

$$\epsilon = \beta(T_0 - T_\infty) \quad (12)$$

which is a measure of the magnitude of temperature variation in the flow field. The coefficient of volumetric expansion  $\beta$  is generally of the order of magnitude between  $10^{-2}$  and  $10^{-4}$  (see table 15 of ref. 7, for example) and for gases,  $\beta = 1/T$ . (Thus, for gases, if  $\beta$  is taken to be constant,  $\epsilon = (T_0 - T_\infty)/T_\infty$ ; that is,  $\epsilon$  is the relative temperature difference.) The coefficient  $\beta$  will be assumed constant. Because in the steady state flow ensues only when there is a temperature

variation in the fluid, the free-convection velocity should then depend directly on  $\epsilon$ , and the variations in pressure and density (from the static,  $\epsilon = 0$ , case) due to the temperature differences should also depend on  $\epsilon$ . Thus

$$U_i = \epsilon \left( \frac{\rho_\infty f_x l^2}{\mu_\infty} \right) u_i \quad (13)$$

$$P = P_s + P_\infty \epsilon \sigma \quad (14)$$

$$\rho = \rho_s + \rho_\infty \epsilon \varphi \quad (15)$$

$$T = T_\infty (1 + \epsilon \theta) \quad (16)$$

where  $-f_x$  denotes the  $X_1$ -component of the body force per unit mass,  $u_i$ ,  $\sigma$ ,  $\varphi$ , and  $\theta$  denote dimensionless functions (which, in general, can be functions of  $\epsilon$ ),  $l$  is some characteristic length (for example, the distance from the edge of the plate to the point of interest),  $P_s$  and  $\rho_s$  are the pressure and the density, respectively, for the static case ( $U_i = 0$  or  $\epsilon = 0$ ), and  $P_\infty$  and  $\rho_\infty$  denote constant values of the pressure and the density (that is, the values if no force field were present) defined by the state equation (in the case of a gas, in particular,  $P_\infty = \rho_\infty R T_\infty$ ): Because there is no characteristic velocity associated with the type of flow under consideration, the velocity is dimensionalized by the factor given in parentheses on the right side of equation (13).

In order to determine the static quantities, it will at first be convenient to consider the particular case of a gas. The problem is then considered with the temperature uniform throughout the flow field at the value  $T_\infty$  (therefore there will be no flow and  $U_i = 0$ ). For this situation, equations (4b) and (6) become

$$P_s = \rho_s R T_\infty \quad (17)$$

and

$$\left. \begin{aligned} \frac{\partial P_s}{\partial X_1} + \rho_s f_x &= 0 \\ \frac{\partial P_s}{\partial X_2} &= 0 \end{aligned} \right\} \quad (18)$$

(It should be noted that eq. (18) expresses the physical fact previously stated that the body force and hydrostatic pressure are in equilibrium for the static case.) Substitution of equation (17) into equation (18) leads to

$$P_s = P_\infty \exp \left( -\frac{f_x}{R T_\infty} X_1 \right) \quad (19)$$

and equation (19) together with equation (17) and the equation defining  $P_\infty$  and  $\rho_\infty$  yields

$$\rho_s = \rho_\infty \exp \left( -\frac{f_x}{R T_\infty} X_1 \right) = \rho_\infty \exp \left( -\frac{f_x \rho_\infty}{P_\infty} X_1 \right) \quad (20)$$

If the exponential in equation (20) is expressed in terms of its series expansion, that equation becomes

$$\rho_s = \rho_\infty \left( 1 - \frac{\rho_\infty f_x}{P_\infty} X_1 + \dots \right) \quad (21)$$

A computation of the second term in the parentheses of equation (21) for the case of air under normal conditions with  $f_x = g$  and the fact that  $X_1$  is of the order of magnitude  $l$  show that  $\rho_\infty g l / P_\infty \sim 10^{-5} l / \text{foot}$ . For the type of problem under consideration,  $l$  will always be of unit order of magnitude so that even if the body force  $f_x$  represents a centrifugal force many times that of gravity, the inequality  $\rho_\infty f_x X_1 / P_\infty \ll 1$  may still be satisfied. Thus, in the subsequent development it will be assumed that  $\rho_s \cong \rho_\infty$ . This assumption, which was justified by the computation for the case of a gas, is expected to be reasonable for other fluids as well. The physical interpretation of this assumption is that under static conditions ( $\epsilon \cong 0$ ), the density (or pressure) is not affected by the force field.

In order that all quantities in the following equations be dimensionless, it is further necessary to define  $x_i = X_i / l$ , where the  $x_i$  are now dimensionless space coordinates. Substituting these new coordinates along with equations (13) to (16) into equations (1), (6), (7), and (4a) and noting equations (18) and that  $\rho_s \cong \rho_\infty$  yield, on neglectation of terms of higher order in  $\epsilon$  compared with those of order  $\epsilon$ ,

$$\frac{\partial u_1}{\partial x_1} + \frac{\partial u_2}{\partial x_2} = 0 \quad (22)$$

$$Gr \left( u_1 \frac{\partial u_1}{\partial x_1} + u_2 \frac{\partial u_1}{\partial x_2} \right) = \Delta u_1 - N Gr \frac{\partial \sigma}{\partial x_1} - \varphi \quad (23)$$

$$Gr \left( u_1 \frac{\partial u_2}{\partial x_1} + u_2 \frac{\partial u_2}{\partial x_2} \right) = \Delta u_2 - N Gr \frac{\partial \sigma}{\partial x_2} \quad (24)$$

$$Gr Pr \left( u_1 \frac{\partial \theta}{\partial x_1} + u_2 \frac{\partial \theta}{\partial x_2} \right) = \frac{\gamma}{\gamma - 1} Gr Pr \left( u_1 \frac{\partial \sigma}{\partial x_1} + u_2 \frac{\partial \sigma}{\partial x_2} \right) + \Delta \theta \quad (25)$$

$$d\varphi = K P_\infty d\sigma - \beta T_\infty d\theta \quad (26)$$

where  $P_\infty / \rho_\infty f_x l = N Gr$  and the Grashof number  $Gr$  and the Prandtl number  $Pr$  are defined as

$$Gr = \frac{\rho_\infty^2 f_x l^3 \epsilon}{\mu_\infty^2}$$

and

$$Pr = \frac{c_p \mu_\infty}{k_\infty}$$

Physically speaking, the Grashof number represents the ratio of the body forces to the viscous forces. The free-convection flows of interest here are those associated with large Grashof numbers. The factors  $K$  and  $\beta$  in equation (26) may well be taken to be constants (see ref. 6).

The boundary conditions (eqs. (8) to (11)) in terms of the new dimensionless variables are

$$u_1(x_1, 0) = u_2(x_1, 0) = 0 \quad (27)$$

$$\theta(x_1, 0) = \frac{1}{\beta T_\infty} \quad (28)$$

$$u_1(x_1, \infty) = 0 \quad (29)$$

$$\theta(x_1, \infty) = 0 \quad (30)$$

Thus, to a first approximation, equations (22) to (26) together with the boundary conditions replace the original equations and boundary conditions. (Note that for gases,  $\beta T_\infty = 1$ .)

The prime assumption made in this analysis is that the higher-order terms in  $\epsilon$  are negligible, which implies that  $\epsilon$  is small, and consequently, that the temperature difference or  $\beta$  is moderately small. It is a consequence of this assumption alone that the basic equations were simplified to equations (22) to (26), wherein the viscosity term in the energy equation is neglected and the only coupling of the momentum and energy equations occurs by means of the body-force term in equation (23). As a result of this assumption, the variations of the viscosity and heat-conductivity coefficients with temperature are also negligible. Without any discussion, the authors of reference 2 start directly from simplified equations of the same form wherein the pressure terms in the energy equation were also neglected. In reference 3 some intuitive arguments are given to justify the simplified equations.

It is now convenient to revert to the more familiar notation where  $x = x_1$ ,  $y = x_2$ ,  $u = u_1$ , and  $v = u_2$ . Equation (22) implies the existence of a stream function  $\psi$  such that

$$\left. \begin{aligned} u &= \frac{\partial \psi}{\partial y} = \psi_y \\ v &= -\frac{\partial \psi}{\partial x} = -\psi_x \end{aligned} \right\} \text{and} \quad (31)$$

where subscripts denote differentiation. Applying equation (31) to equations (23) to (25) yields, respectively,

$$\frac{1}{Gr} (\Delta \psi_y - \varphi) = \psi_y \psi_{yy} - \psi_x \psi_{xy} + N \sigma_x \quad (32)$$

$$-\frac{1}{Gr} (\Delta \psi_x) = -\psi_y \psi_{xx} + \psi_x \psi_{xy} + N \sigma_y \quad (33)$$

$$\frac{1}{Gr Pr} (\Delta \theta) = \psi_y \theta_x - \psi_x \theta_y - \frac{\gamma}{\gamma - 1} (\psi_y \sigma_x - \psi_x \sigma_y) \quad (34)$$

The boundary conditions (eqs. (27) to (30)) become

$$\psi_y(x, 0) = \psi_x(x, 0) = 0 \quad (35)$$

$$\theta(x, 0) = \frac{1}{\beta T_\infty} \quad (36)$$

$$\psi_y(x, \infty) = \theta(x, \infty) = 0 \quad (37)$$

Equations (32) to (34) and equation (26) form the system of equations for the four unknown functions  $\psi$ ,  $\theta$ ,  $\varphi$ , and  $\sigma$  of the problem. The system is nonlinear, and therefore

further simplification of the equations would be desirable. Just as in the case of forced-convection flows where the Reynolds number determines the type of flow or, in mathematical terms, the type of solution, the Grashof number is the prime factor for free-convection flows. For the case of small Grashof number, it can be seen from equations (32) to (34) that a perturbation in the small parameter  $Gr$  will yield a system of linear equations. For Grashof numbers of unit order of magnitude, no further important simplification can be made and the solutions would have to be obtained numerically. For the other limiting case, that of large Grashof numbers (which is the case under consideration herein), it would, at first thought, appear that some simplification could be obtained by performing a perturbation in the small parameter  $1/Gr$ . However, this would then imply that the term containing the highest-order derivatives (the left term in equations (32) to (34)) could, among others, be neglected. (This argument would also imply that the body-force term  $\varphi$  in equation (32), which is essentially causing the flow, could also be neglected.) The omission of the highest-order derivatives from consideration, however, would lead to solutions which would not satisfy all the boundary conditions. Problems of this type are referred to as singular perturbation problems. For further discussions of singular perturbation problems, see references 8 and 9.

Equations in which a small parameter multiplies the highest-order terms are said to be of the boundary-layer type, because in order for solutions which satisfy all the boundary conditions to be obtained, the highest-order terms must be considered near the boundary. This fact implies the existence of a thin region, called the boundary layer, wherein the functions vary rapidly from the value at the boundary to that in the flow outside this layer. The conclusion to be drawn from the preceding discussion is that for large Grashof numbers the flow is of the boundary-layer type. Schmidt and Beckmann (ref. 2) also made the boundary-layer assumptions in their theoretical development, and these assumptions were justified on the basis of their experimental observations. The Grashof numbers for their experiments were of the order of  $8 \times 10^6$ .

In view of the fact, previously discussed, that highest-order derivatives of each dependent variable as well as of those terms of physical importance (as, for example, the body-force term) must be retained in the boundary layer, it is convenient to make both sides of each of the equations of the same order in  $Gr$ . In this way, as will be shown, the equations will be further simplified. It is thus convenient to make the following transformations in the system of equations (32) to (34) and (26) and then to retain only the dominant parts (that is, those multiplied by  $Gr$  to the highest power) of each individual term.

Let  $\bar{y} = Gr^r y$ ,  $\bar{\psi} = Gr^s \psi$ ,  $\bar{\sigma} = Gr^t \sigma$ ,  $\bar{\varphi} = \varphi$ , and  $\bar{\theta} = \theta$ . Then equations (32) to (34) and (26) become

$$Gr^{s+3r-1} \bar{\psi}_{\bar{y}\bar{y}} - Gr^{-1} \bar{\varphi} = Gr^{2s+2r} (\bar{\psi}_y \bar{\psi}_{\bar{y}} - \bar{\psi}_x \bar{\psi}_{\bar{y}}) + N Gr^t \bar{\sigma}_x \quad (38)$$

$$-Gr^{s+2r-1} \bar{\psi}_{\bar{y}\bar{y}} = Gr^{2s+r} (-\bar{\psi}_y \bar{\psi}_{\bar{y}} + \bar{\psi}_x \bar{\psi}_{\bar{y}}) + N Gr^{t+r} \bar{\sigma}_y \quad (39)$$

$$\frac{Gr^{2r-1}}{Pr} \bar{\theta}_{\bar{y}\bar{y}} = Gr^{s+r} (\bar{\psi}_y \bar{\theta}_x - \bar{\psi}_x \bar{\theta}_y) - \frac{\gamma}{\gamma-1} Gr^{t+s+r} (\bar{\psi}_y \bar{\sigma}_x - \bar{\psi}_x \bar{\sigma}_y) \quad (40)$$

$$d\bar{\varphi} = KP_\infty Gr^t d\bar{\sigma} - \beta T_\infty d\bar{\theta} \quad (41)$$

It now can be seen that by proper choice of  $r$ ,  $s$ , and  $t$  a transformation of the type given provides a means for making the important terms in the differential equations of the same order in  $Gr$ . Thus if  $r = 1/2$ ,  $s = -1/2$ , and  $t = -1$ , equations (38) to (41) become

$$\bar{\psi}_{\bar{y}\bar{y}} - \bar{\varphi} = \bar{\psi}_y \bar{\psi}_{\bar{y}} - \bar{\psi}_x \bar{\psi}_{\bar{y}} + N \bar{\sigma}_x \quad (42)$$

$$N \bar{\sigma}_y = O(Gr^{-1/2}) \approx 0 \quad (43)$$

$$\bar{\theta}_{\bar{y}\bar{y}} = Pr (\bar{\psi}_y \bar{\theta}_x - \bar{\psi}_x \bar{\theta}_y) \quad (44)$$

$$d\bar{\varphi} + \beta T_\infty d\bar{\theta} = 0 \quad (45)$$

More generally, if  $N$  is very much different from unit order of magnitude, a value of  $t$  can always be chosen (depending on  $N$ ) such that equations (42) to (45) are obtained. (For any negative  $t$  less than  $-1$ , the last term of eq. (42) will also disappear.)

There are now several important points to be discussed concerning the transformation just made and the resulting simplified equations. First, it should be noted that the transformation is merely a formal expression of the boundary-layer assumptions first made by Prandtl and hence the solutions will be asymptotic for large  $Gr$ . Second, the second equation of motion here also reduces to state that the pressure across the boundary layer is constant. Third, the pressure terms in the energy and state equations are here found to be negligible. This fact verifies a priori assumptions made by others from the physics of the problem. Finally, note that integration of the general state equation (independent of pressure) as now given by equation (45) leads to

$$\bar{\varphi} + \beta T_\infty \bar{\theta} = 0 \quad (46)$$

where the constant of integration has been taken as zero without any loss of generality. For the particular case of a gas,  $\beta = 1/T_\infty$  so that equation (46) becomes

$$\bar{\varphi} + \bar{\theta} = 0$$

The boundary conditions (eqs. (35) to (37)) now can be written

$$\bar{\psi}_y(x, 0) = \bar{\psi}_x(x, 0) = 0 \quad (47)$$

$$\bar{\theta}(x, 0) = \frac{1}{\beta T_\infty} \quad (48)$$

$$\bar{\psi}_y(x, \infty) = \bar{\theta}(x, \infty) = 0 \quad (49)$$

If now it is assumed that  $\bar{\sigma}_x = 0$  in equation (42) since consideration is here being given to a flat plate, and if  $\bar{\varphi}$  is eliminated from equation (42) by use of equation (46), there results the system of equations

$$\bar{\psi}_{xy} + \beta T_{\infty} \bar{\theta} = \bar{\psi}_y \bar{\psi}_{xx} - \bar{\psi}_x \bar{\psi}_{yy} \quad (50)$$

$$\bar{\theta}_{xy} = Pr(\bar{\psi}_y \bar{\theta}_x - \bar{\psi}_x \bar{\theta}_y) \quad (51)$$

Thus the problem has been reduced to the solution of the two simultaneous partial differential equations (eqs. (50) and (51)) subject to the boundary conditions (eqs. (47) to (49)).

Final simplification of the equations is made by application of the so-called similarity transformation of boundary-layer theory. Thus, let

$$\eta = \frac{\bar{y}}{(4x)^{\frac{1}{2}}} \quad (52)$$

and

$$\bar{\psi} = (4x)^{\frac{1}{2}} F(\eta) \quad (53)$$

$$\bar{\theta} = \frac{H(\eta)}{\beta T_{\infty}} \quad (54)$$

Then equations (50) and (51) are reduced to the following ordinary differential equations:

$$F''' + 3FF'' - 2F'^2 + H = 0 \quad (55)$$

$$H'' + 2Pr FH' = 0 \quad (56)$$

where the primes denote differentiations with respect to  $\eta$ . The reciprocal one-fourth power similarity as given in equation (52) is characteristic of free-convection flows just as the reciprocal square-root type is characteristic of the forced-convection flows. The boundary conditions become

$$F'(0) = F(0) = 0 \quad (57)$$

$$H(0) = 1 \quad (58)$$

$$F'(\infty) = H(\infty) = 0 \quad (59)$$

The use of a transformation like equation (52) essentially specifies an additional boundary condition, namely, that the conditions to be satisfied at  $y = \infty$  (or  $\eta = \infty$ ) should also be satisfied at  $x = 0$ . It is for this reason that the flows previously discussed which would flow toward the edge (downward) are not amenable to this type of analysis, for such flows would violate this additional condition, which essentially states that the boundary-layer development starts at the edge of the plate.

#### SOLUTION OF THE BOUNDARY-VALUE PROBLEM

The solutions of the simplified equations (55) and (56), satisfying the boundary conditions as given by equations (57) to (59), were obtained by use of an IBM Card-Programmed Electronic Calculator. A detailed account of the procedure followed in the determination of the unknown functions is presented in appendix B by Dr. Lynn U. Albers. The functions  $F$  and  $H$  together with their derivatives are given in table I for Prandtl numbers of 0.01, 0.72, 0.733, 1, 2, 10, 100, and 1000. Even though the Prandtl number for air is taken as 0.72 in this report, the solutions for  $Pr = 0.733$  were also computed and are presented as a check with the

Schmidt-Beckmann calculations wherein the value of Prandtl number of 0.733 was used. The particular values of the Prandtl numbers given were chosen to correspond to those for liquid metals, gases, liquids (such as water and oil), and very viscous liquids (such as glycerin or oils at very low temperatures).

## RESULTS

### VELOCITY AND TEMPERATURE DISTRIBUTIONS

By means of the various transformations made in the analysis it can easily be verified that

$$\frac{U}{2\sqrt{\beta(T_0 - T_{\infty})} f_x X} = \frac{v_{\infty}}{2\sqrt{Gr_x}} = F'(\eta) \quad (60)$$

and

$$\left(\frac{T - T_{\infty}}{T_0 - T_{\infty}}\right) = H(\eta) \quad (61)$$

where

$$\eta = \left[\frac{f_x(T_0 - T_{\infty})\beta}{4v_{\infty}^2 X}\right]^{\frac{1}{4}} Y = \left(\frac{Gr_x}{4}\right)^{\frac{1}{4}} \frac{Y}{X} \quad (62)$$

Equations (60) to (62) relate the physical quantities to the dimensionless functions  $F$  and  $H$  which are now known. The dimensionless velocity and temperature distributions as given by equations (60) and (61) are presented in figures 1 and 2, respectively, as functions of  $\eta$  for the various values of Prandtl number. The computations made here agree with those for  $Pr = 0.733$  as given in reference 2 up to the third significant figure. For  $Pr = 10, 100, \text{ and } 1000$ , the present results agree in general with those of reference 3. Since only curves are presented in reference 3, the precision of the agreement cannot be stated.

The maximum values of the dimensionless velocity distributions occur at larger values of the argument  $\eta$  as the Prandtl number decreases and the velocities decrease with increasing  $Pr$ . It should also be noted that the dynamic and thermal boundary-layer thicknesses can be estimated from the abscissas of figures 1 and 2, respectively, and that for  $Pr \gg 1$  the velocity boundary layer is much thicker than the thermal boundary layer.

The occurrence of  $f_x$  (or  $Gr_x$  as given by eq. (60)), which may be very large for flows generated by centrifugal forces, in the denominator of the ordinate implies that velocities of appreciable magnitude can be associated with such free-convection flows. In particular, if  $f_x = 10^6$  feet per second squared, which is a reasonable conservative figure for present-day rotating systems,  $\epsilon = 0.2$  (which is within the limits of the theory presented herein), and arbitrarily  $X = 0.25$  foot, then the maximum velocity attained at a Prandtl number of 0.72 is approximately 125 feet per second. This value of the maximum velocity could, of course, be doubled or even tripled under the proper conditions. One limitation to a calculation of this sort, as can be seen by comparison of the denominators of the left and middle terms of equation (60), should be kept in mind; namely, the limiting Grashof number for laminar flows. In lieu of a complete stability

analysis on this type of flow, this limiting value is taken to be  $10^9$ , as indicated in reference 10. Consideration of this limitation then implies (see eq. (60)) that for large laminar velocities either  $\nu_\infty$  must be large or  $X$  must be small.

COMPARISON WITH EXPERIMENTS

Careful experiments of free-convection flows (as generated by gravitational forces) about vertical flat plates were made by Schmidt and Beckmann (ref. 2) in which velocity measurements at various points along the plate were made by means of a quartz-filament anemometer and the temperature measurements were obtained by means of manganese-constantan thermocouples. Eckert (ref. 1) performed similar experiments in which the measurements were made by means of a

Zehnder-Mach interferometer. The results of both sets of experiments are in good agreement, but since the data presented in reference 2 by Schmidt and Beckmann appear in more detail, these data will be used for comparison with the theory.

The experiments of reference 2 were performed on two different (in that the edges were smoothed either symmetrically or not) 12- by 25-centimeter plates and on one 50- by 50-centimeter plate. It should here be pointed out that the results for the two smaller plates were almost identical and that the flow was entirely laminar except near the outer edge of the boundary layer where the slight turbulence of the room air disturbed the measurements somewhat. (This effect was also observed by Eckert.) Large periodic oscillations of the flow near the downstream edge of the larger plate were observed in addition to the slight turbulence near the

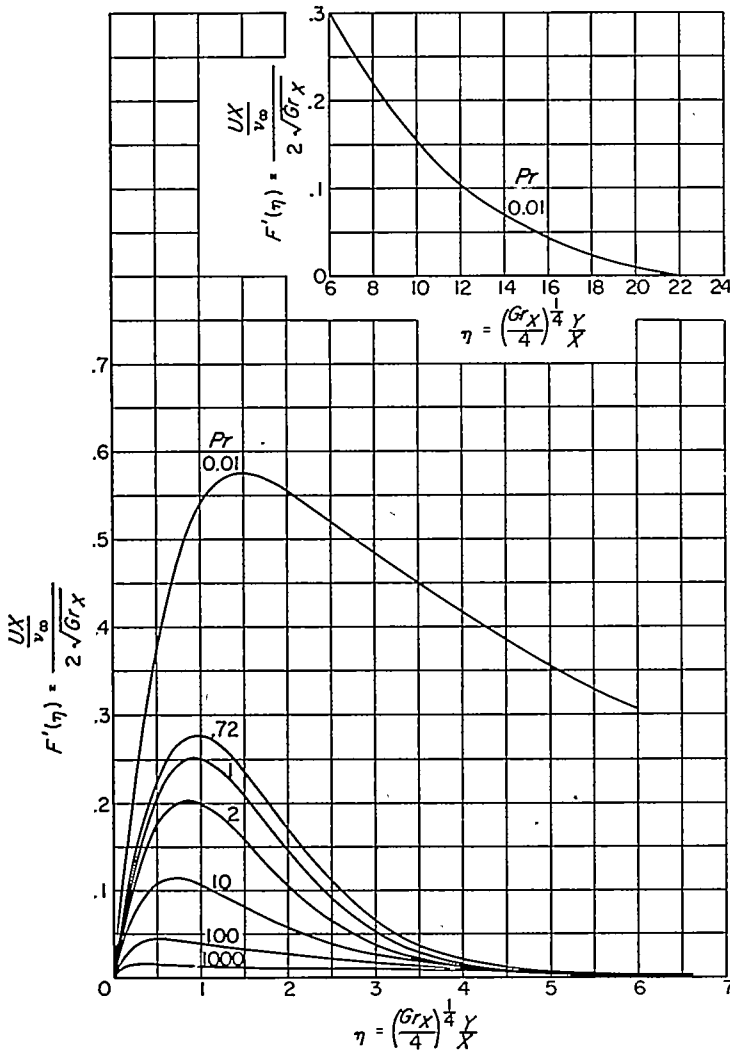


FIGURE 1.—Dimensionless velocity distributions for various Prandtl numbers.

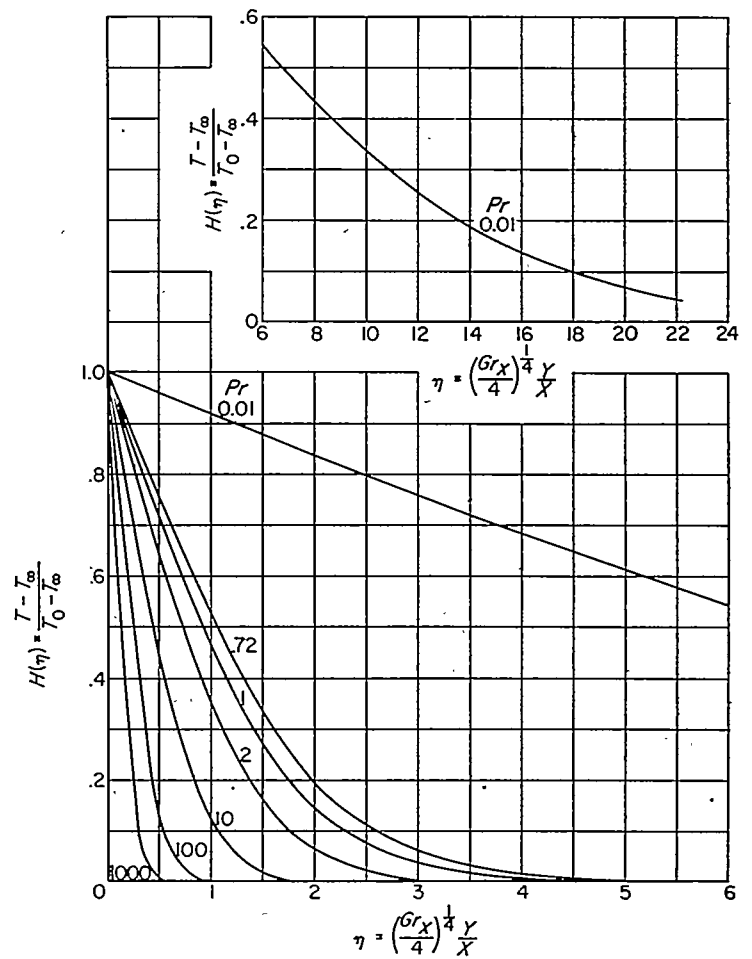


FIGURE 2.—Dimensionless temperature distributions for various Prandtl numbers.

outer edge of the boundary layer. Hence the data from the larger plate should not be expected to yield completely satisfactory agreement with the laminar theory as presented here.

Since the physical quantities can be expressed in terms of a single variable as in equations (60) and (61), it is to be expected that the data taken at the various points along the plates should all lie on a single line if the data are correlated according to equations (60) and (61). Thus for the smaller plates where  $(T_0 - T_\infty) = 95.22^\circ \text{R}$  and  $T_\infty = 518.68^\circ \text{R}$ , equations (60) to (62) become

$$\frac{U}{4.862\sqrt{X}} = F'(\eta) \quad (63)$$

$$\frac{T - 518.68}{95.22} = H(\eta) \quad (64)$$

$$\eta = 88.26 \frac{Y}{X^{3/4}} \quad (65)$$

The velocity and temperature distributions are so plotted in figures 3 and 4, respectively, as are the curves computed theoretically for  $Pr = 0.72$ . It can be seen that the agreement is in general very good for small values of  $\eta$  and somewhat less satisfactory though still rather good for the larger values of  $\eta$ . The scatter in the range of the larger values of  $\eta$  is believed to be caused by the previously discussed room

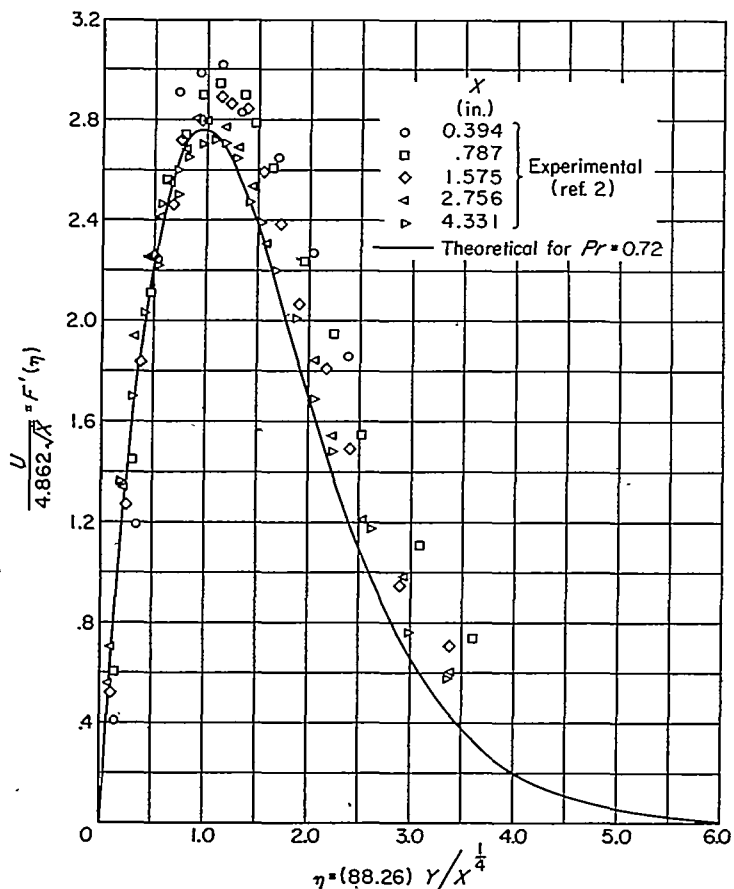


FIGURE 3.—Comparison of small plate experimental and theoretical velocity distributions for Prandtl number of 0.72.

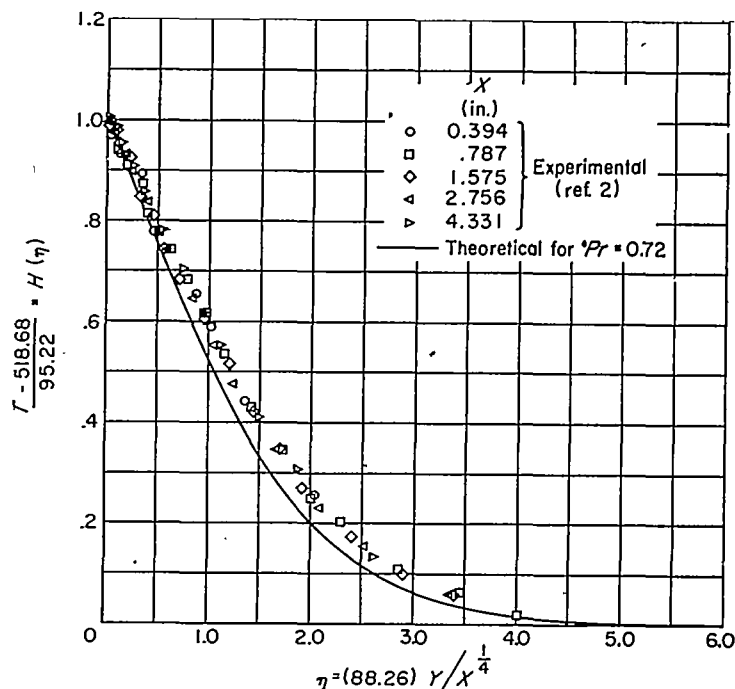


FIGURE 4.—Comparison of small plate experimental and theoretical temperature distributions for Prandtl number of 0.72.

turbulence. It should also be noted that the points farthest away from the theoretical are those measured near the leading edge. These points should not, of course, be expected to agree too well with the theory since the boundary-layer assumptions made in the theoretical development imply that the distance along the plate is large as compared with the boundary-layer thickness. Hence, this assumption is invalid near the leading edge. Schmidt and Beckmann obtained closer agreement between the theory and the experiments for the temperature data and poorer agreement for the velocity data by basing the kinematic viscosity coefficient in equation (62) on the plate temperature rather than on the undisturbed stream temperature as was done here.

For the larger plate,  $(T_0 - T_\infty) = 83.7^\circ \text{R}$  and  $T_\infty = 527.14^\circ \text{R}$ , so that equations (60) to (62) become

$$\frac{U}{4.522\sqrt{X}} = F'(\eta) \quad (66)$$

$$\frac{T - 527.14}{83.7} = H(\eta) \quad (67)$$

$$\eta = 83.93 \frac{Y}{X^{3/4}} \quad (68)$$

The velocity and temperature distributions for this experiment are plotted in figures 5 and 6, respectively, and again the theoretical curves for  $Pr = 0.72$  are included. In figure 5 it can be seen that for large  $\eta$  the agreement is rather poor, particularly for the data for both small and large values of  $X$ . The poor agreement for small values of  $X$  is again due to the theory limitation near the edge of the plate and for large values of  $X$ , to the fact that the flow was becoming turbulent there.



FLOW AND HEAT-TRANSFER PARAMETERS

In addition to the velocity and temperature distributions, it is often desirable to compute other physically important quantities (such as shear stress, drag, heat-transfer rate, and heat-transfer coefficient) associated with the free-convection flow. To this end, two parameters, a flow parameter and a heat-transfer parameter, are derived in appendixes C and D, respectively.

The flow parameter

$$\frac{\tau}{(4Gr_x^3)^{1/4}(\nu_\infty\mu_0/X^2)} = F''(0)$$

is presented as a function of Prandtl number in figure 7. Thus, the various flow quantities for a given set of conditions can easily be computed by application of figure 7.

The local heat-transfer parameter

$$\frac{Nu}{(Gr_x/4)^{1/4}} = -H'(0)$$

as determined here is given as a function of Prandtl number in figure 8. A calculation of the local Nusselt number from this equation for  $Pr=0.72$  and  $Gr_x=10^9$  yields a value of 63.5, which indicates that large heat-transfer coefficients can also be obtained with free-convection flows.

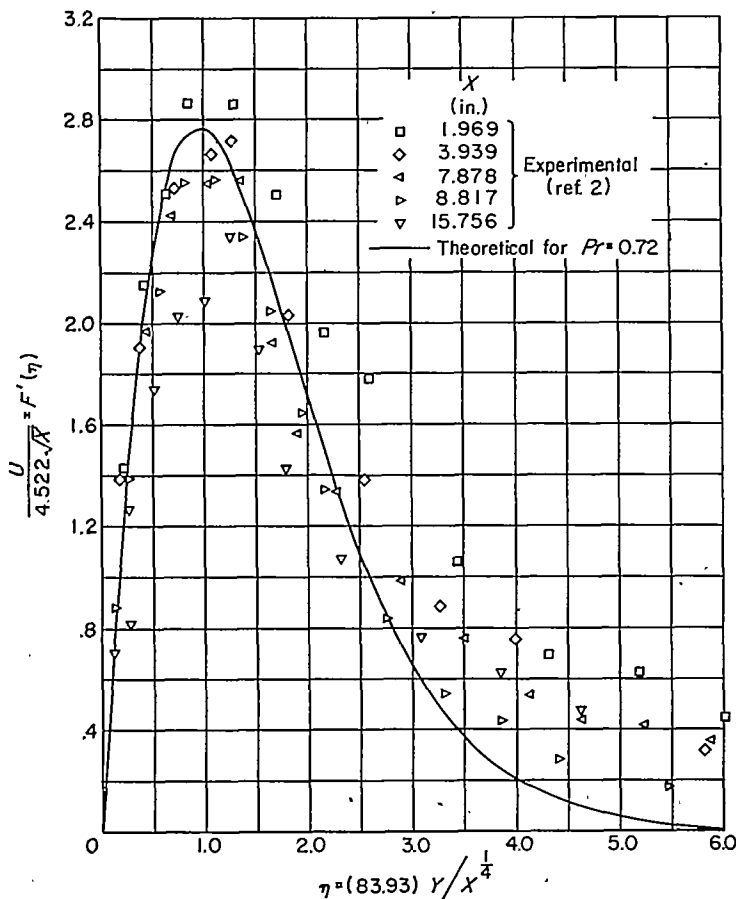


FIGURE 5.—Comparison of large plate experimental and theoretical velocity distributions for Prandtl number of 0.72.

On the basis of a simplified theory (that is, by use of integrated momentum and energy equations and assumed velocity and temperature distributions), Eckert (see p. 162 of ref. 7) obtained the approximate relation

$$\frac{Nu}{(Gr_x/4)^{1/4}} = \frac{0.718(Pr)^{1/4}}{(0.952 + Pr)^{1/4}}$$

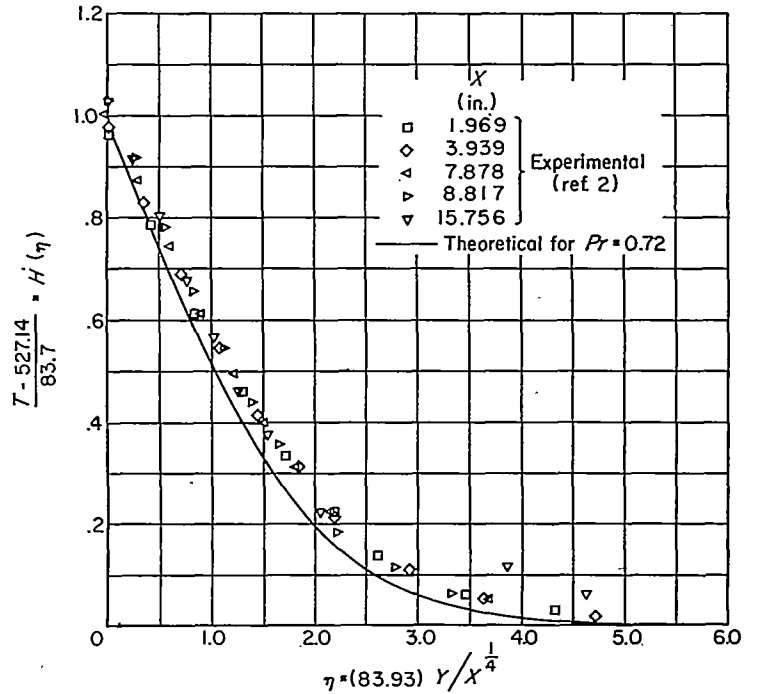


FIGURE 6.—Comparison of large plate experimental and theoretical temperature distributions for Prandtl number of 0.72.

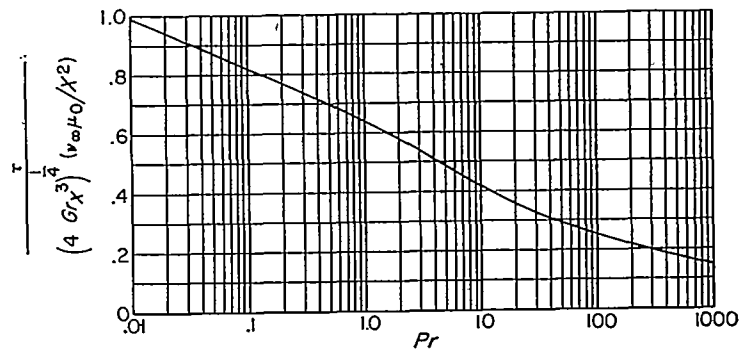


FIGURE 7.—Dimensionless flow parameter as function of Prandtl number.

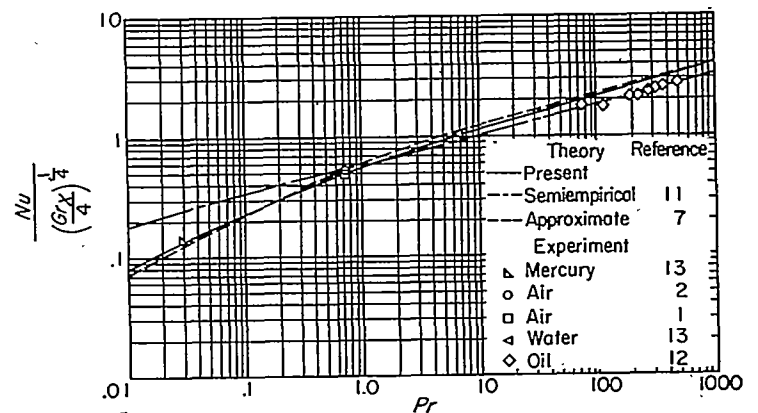


FIGURE 8.—Dimensionless heat-transfer parameter as function of Prandtl number.

The curve representing this equation is also presented in figure 8, and it closely approximates (to within about 10 percent) the curve determined by the more exact considerations of this report over the entire Prandtl number range. A semiempirical equation as given in reference 11 relating the average (over the length  $X$ ) Nusselt number to the Prandtl and Grashof numbers which has been used in the heat-transfer calculations up to the present is

$$Nu_{av} = 0.548 [(Pr)Gr]^{\frac{1}{4}}$$

The constant 0.548 pertains specifically to air; for oil it should be 0.555 (see ref. 12) and for mercury, approximately 0.33 (see ref. 13). In order to obtain local values from the average ones given by the last equation, it is merely necessary to multiply the average values by 0.75. (The determination of this reduction factor of 0.75 is discussed in appendix D.) Thus in terms of the local quantities the semiempirical relation becomes

$$Nu = 0.411 [(Pr)Gr_x]^{\frac{1}{4}}$$

or

$$\frac{Nu}{(Gr_x/4)^{\frac{1}{4}}} = 0.581 (Pr)^{\frac{1}{4}}$$

The curve given by this equation is also presented in figure 8 and the agreement with the theoretical curve is very good for Prandtl numbers near unity, not so good for large Prandtl numbers, and very poor for the small Prandtl numbers. Of course, changes of the constants in the semiempirical relation as previously discussed for the large or small Prandtl number cases (oil and mercury, respectively, for example) would cause the semiempirical curve to approximate the theoretical curve more closely. The values of the heat-transfer parameter obtained experimentally for mercury ( $Pr=0.03$ ), air ( $Pr=0.72$ ), water ( $Pr=7$ ), and oil ( $Pr=75.5, 115, 190, 224, 275, 318, 368, \text{ and } 442$ ) are here reduced by the factor 0.75 from the average values reported. The value for mercury is an average taken of four readings from a curve, since this experiment was the only one not reported in tabular form. From figure 8 it can be seen that all of the experimental values except those for the oil experiments are in very good agreement with the theoretically computed values. The

data from the oil experiments, though not so good, show reasonable agreement (maximum error of approximately 20 percent) with the theoretical curve and good agreement, as is to be expected, with the semiempirical curve. The difference between the theoretical values and the oil experiment results can possibly be due to the fact that the viscosity changes in oil are large even for small temperature differences or due to the end effects in the measurements.

#### CONCLUSIONS

An analysis was made of the free-convection flow about a flat plate oriented in a direction parallel to that of the generating body force under the prime assumption that the relative temperature difference is small. It was found that the Grashof number was the principal factor determining the type of flow and that for large Grashof numbers the flow was of the boundary-layer type. The theoretical development was then continued to consider only the cases of large Grashof number because these are of most importance in aeronautics.

Velocity and temperature profiles for Prandtl numbers of 0.01, 0.72, 0.733, 1, 2, 10, 100, and 1000 were computed on the basis of a constant body force and plate temperature and agreement with experiments where the fluid was air (Prandtl number of 0.72) was good. It was also demonstrated that velocities and Nusselt numbers of the order of magnitude of those obtained in forced-convection could be obtained in free-convection flows.

A flow parameter and a heat-transfer parameter which are functions of the Prandtl number alone were derived. Calculations of the important physical quantities such as shear stress, heat-transfer rate, and the like can be computed from these parameters. Values of the heat-transfer parameter obtained from an approximate theoretical development and from experiments compared with values computed from the present development showed good agreement over a wide range of Prandtl number (0.01 to 1000). It is shown that the commonly used semiempirical relation for the heat-transfer coefficient will yield good results only in restricted Prandtl number ranges.

LEWIS FLIGHT PROPULSION LABORATORY

NATIONAL ADVISORY COMMITTEE FOR AERONAUTICS  
CLEVELAND, OHIO, October 3, 1951

## APPENDIX A

### SYMBOLS

The following notation is used in this report:

$A_i^{(n)}, B_j^{(n)}, C^{(n)}, D_i^{(n)}$	coefficients in numerical differentiation and integration formulas
$c_p$	specific heat at constant pressure
$F$	dimensionless velocity function
$f_i$	components of body force per unit mass, $i=1, 2, 3$
$f_x$	negative of $X$ -component of body force per unit mass

$Gr$	Grashof number, $\frac{\rho_{\infty}^2 \int_x l^3 \epsilon}{\mu_{\infty}^2}$
$Gr_x$	Grashof number based on $X$
$g$	gravitational force per unit mass (or acceleration due to gravity)
$H$	dimensionless temperature function
$h$	heat-transfer coefficient
$K$	isothermal compressibility coefficient, $-\rho \left[ \frac{\partial (1/\rho)}{\partial P} \right]_T$

$k$	thermal-conductivity coefficient
$l$	characteristic length
$m, n$	arbitrary exponents
$N$	a number, defined following equation (26)
$Nu$	Nusselt number, $hX/k$
$Nu_{av}$	average Nusselt number
$P$	pressure
$Pr$	Prandtl number
$R$	gas constant
$r, s, t$	arbitrary exponents
$T$	absolute temperature
$U_i$	velocity components, $i=1, 2, 3$
$u_i$	dimensionless velocity components, $i=1, 2, 3$
$u$	dimensionless velocity component in $x$ -direction
$v$	dimensionless velocity component in $y$ -direction
$X_i$	Cartesian coordinates, $i=1, 2, 3$
$x_i$	dimensionless Cartesian coordinates, $i=1, 2, 3$
$x$	dimensionless Cartesian coordinate
$Y$	Cartesian coordinate
$y$	dimensionless Cartesian coordinate

$\beta$	coefficient of volumetric expansion, $\rho \left[ \frac{\partial (1/\rho)}{\partial T} \right]_p$
$\gamma$	ratio of specific heats
$\Delta$	Laplacian operator
$\epsilon$	relative temperature difference, $\beta(T_0 - T_\infty)$
$\eta$	similarity variable
$\theta$	dimensionless temperature function
$\kappa$	step size used in numerical calculations
$\mu$	absolute viscosity
$\nu$	kinematic viscosity
$\rho$	density
$\sigma$	dimensionless pressure function
$\tau$	shear stress
$\varphi$	dimensionless density function
$\psi$	stream function
Subscripts:	
$i, j$	Cartesian tensor and summation subscripts
$s$	denotes evaluation at static conditions ( $\epsilon=0$ )
$0$	denotes evaluation at plate surface
$\infty$	denotes evaluation at undisturbed conditions
Subscript notation is used to denote partial differentiation.	
Superscripts:	
Primes denote ordinary differentiation.	
Bars (as $\bar{\sigma}$ or $\bar{\eta}$ ) denote transformed dimensionless quantities.	

## APPENDIX B

### NUMERICAL SOLUTION OF SIMPLIFIED BOUNDARY-VALUE PROBLEM

By LYNN U. ALBERS

The method is presented herein by which solutions to the boundary-value problem

$$F''' + 3FF'' - 2F'^2 + H = 0 \quad (B1)$$

$$H'' + 3PrFH' = 0 \quad (B2)$$

$$F(0) = F'(0) = 0 \quad H(0) = 1$$

$$F'(\infty) = H(\infty) = 0$$

were obtained for the cases of  $Pr$  equal to 0.01, 0.72, 0.733, 1, 2, 10, 100, and 1000. This discussion will enable the results to be clearly evaluated and will perhaps serve as a guide in the numerical solution of similar problems.

Each of the cases of the problem has a solution for a particular set of values for  $F''(0)$  and  $H'(0)$ , hereinafter called eigenvalues. The basic approach to the problem was to estimate the eigenvalues and to integrate out from zero, obtaining functions which satisfied equations (B1) and (B2) at each step. The integration was continued until the functions  $F'$  and  $H$  behaved in a fashion inconsistent with the boundary values at infinity; for example, when they became negative or diverged to infinity. Improved estimates of the eigenvalues were then made on the basis of the results of preceding runs and the process was repeated successively until a solution was obtained.

Modifications required to overcome specific obstacles will be discussed after sufficient details of the basic procedure have been given. Then an evaluation of the accuracy of the numerical results will be made.

The integration process consists of two parts, a starting phase and an extension phase. The starting phase begins with an estimate of the eigenvalues  $F''(0)$  and  $H'(0)$  and a decision on the step size  $\kappa$  to be used. It continues with an iterative process of alternately computing  $F''''$  and  $H''$  at the first four points and integrating them by five-point formulas. This process and that in the extension phases are so arranged that the differential equations are satisfied at each integral multiple of the step size.

The extension phase used preceding data to integrate step by step beyond the fourth point. Diagrams of both phases will be given after a few preliminary explanations.

All integration formulas used are based on the same idea. If a function, for example,  $F''''$ , is known at five points, there is a unique fourth-degree polynomial which agrees with it at these five points. Moreover, if the successive antiderivatives (integrals)  $F'''$ ,  $F''$ , and  $F'$  of  $F''''$  are known at one point, there are unique fifth-, sixth-, and seventh-degree polynomials which are successive antiderivatives of this fourth-degree polynomial and which agree with  $F'''$ ,  $F''$ , and  $F'$ , respectively, at the one point. It is then a simple algebra problem to deduce from the values of  $F''''$  at five points and

$F$ ,  $F'$ , and  $F''$  at a single point the values of any of these four polynomials at any point. These results will approximate the functions  $F$ ,  $F'$ ,  $F''$ , and  $F'''$  to a degree dependent on step size, the relative positions of the points in question, and the magnitude of the fifth derivative of  $F'''$  in the neighborhood of these points.

The preceding algebra problem can be presolved in all situations that arise in the starting and extension phases of the present problem and specific integration formulas may be deduced. These formulas are discussed in the next paragraph.

Let  $F'''$  be denoted at five successive points by  $F_0'''$ ,  $F_1'''$ ,  $F_2'''$ ,  $F_3'''$ , and  $F_4'''$ . In the starting phase, these points are 0,  $\kappa$ ,  $2\kappa$ ,  $3\kappa$ , and  $4\kappa$ , and  $F_0$ ,  $F_0'$ , and  $F_0''$  are also known. Then the five sets of formulas required in the starting phase are.

$$F_i'' = F_0'' + \frac{\kappa}{D_i^{(1)}} \sum_{j=0}^4 A_{ij}^{(1)} F_j''' \quad i=1, 2, 3, 4 \quad (B3)$$

$$H_i' = H_0' + \frac{\kappa}{D_i^{(1)}} \sum_{j=0}^4 A_{ij}^{(1)} H_j'' \quad i=1, 2, 3, 4 \quad (B4)$$

$$F_i' = F_0' + i\kappa F_0'' + \frac{\kappa^2}{D_i^{(2)}} \sum_{j=0}^4 A_{ij}^{(2)} F_j''' \quad i=1, 2, 3, 4 \quad (B5)$$

$$H_i = H_0 + i\kappa H_0' + \frac{\kappa^2}{D_i^{(2)}} \sum_{j=0}^4 A_{ij}^{(2)} H_j'' \quad i=1, 2, 3, 4 \quad (B6)$$

$$F_i = F_0 + i\kappa F_0' + \frac{i^2 \kappa^2}{2} F_0'' + \frac{\kappa^3}{D_i^{(3)}} \sum_{j=0}^4 A_{ij}^{(3)} F_j''' \quad i=1, 2, 3, 4 \quad (B7)$$

where the superscripts on the  $A_{ij}^{(n)}$  and  $D_i^{(n)}$  refer to the order of integration.

The constants  $A_{ij}^{(n)}$  and  $D_i^{(n)}$  may be read from the following tables:

For  $A_{ij}^{(1)}$  and  $D_i^{(1)}$ :

$A_{ij}^{(1)}$						$D_i^{(1)}$
$i \backslash j$	0	1	2	3	4	
1	251	646	-264	106	-19	720
2	29	124	24	4	-1	90
3	27	102	72	42	-3	80
4	14	64	24	64	14	46

For  $A_{ij}^{(2)}$  and  $D_i^{(2)}$ :

$A_{ij}^{(2)}$						$D_i^{(2)}$
$i \backslash j$	0	1	2	3	4	
1	367	540	-282	116	-21	1440
2	53	144	-30	16	-3	90
3	441	1404	162	180	-27	480
4	56	192	48	64	0	45

For  $A_{ij}^{(3)}$  and  $D_i^{(3)}$ :

$A_{ij}^{(3)}$						$D_i^{(3)}$
$i \backslash j$	0	1	2	3	4	
1	1017	1070	-618	253	-47	10080
2	331	664	-240	104	-19	630
3	1431	3726	-486	460	-81	1120
4	744	2176	96	384	-40	315

It is now possible to diagram the steps of the starting phase of the integration. If each bar above a function denotes an improved estimate of it, and the first estimates of  $F_1'''$ ,  $F_2'''$ ,  $F_3'''$ , and  $F_4'''$  are all equal to  $F_0'''$ , and similarly for the  $H''$ , then the starting phase diagrams are

(1)  $(F_0, F_0', F_0'', F_0''', F_1''', F_2''', F_3''', F_4''') \rightarrow F_1, F_1', F_1''$   
 (This diagram means that the values in parentheses are used with appropriate integration formulas from (B3) to (B7) to obtain  $F$ ,  $F'$ , and  $F''$  at  $\eta=\kappa$ .)

(2)  $(H_0, H_0', H_0'', H_1'', H_2'', H_3'', H_4'') \rightarrow H_1, H_1'$

(3)  $(F_1, F_1', F_1'', H_1, H_1') \rightarrow \bar{F}_1''', \bar{H}_1''$

(The preceding diagram means that the values in parentheses are substituted in the differential equations (B1) and (B2) to obtain  $F'''$  and  $H''$  at  $\eta=\kappa$ .)

(4)  $(F_0, F_0', F_0'', F_0''', \bar{F}_1''', F_2''', F_3''', F_4''') \rightarrow F_2, F_2', F_2''$

(5)  $(H_0, H_0', H_0'', \bar{H}_1'', H_2'', H_3'', H_4'') \rightarrow H_2, H_2'$

(6)  $(F_2, F_2', F_2'', H_2, H_2') \rightarrow \bar{F}_2''', \bar{H}_2''$

(7)  $(F_0, F_0', F_0'', F_0''', \bar{F}_1''', \bar{F}_2''', F_3''', F_4''') \rightarrow F_3, F_3', F_3''$

(8)  $(H_0, H_0', H_0'', \bar{H}_1'', \bar{H}_2'', H_3'', H_4'') \rightarrow H_3, H_3'$

(9)  $(F_3, F_3', F_3'', H_3, H_3') \rightarrow \bar{F}_3''', \bar{H}_3''$

(10)  $(F_0, F_0', F_0'', F_0''', \bar{F}_1''', \bar{F}_2''', \bar{F}_3''', F_4''') \rightarrow F_4, F_4', F_4''$

(11)  $(H_0, H_0', H_0'', \bar{H}_1'', \bar{H}_2'', \bar{H}_3'', H_4'') \rightarrow H_4, H_4'$

(12)  $(F_4, F_4', F_4'', H_4, H_4') \rightarrow \bar{F}_4''', \bar{H}_4''$

It may be noted here that all four values of  $F'''$  and  $H''$  have been improved, and further improvement will require iteration of steps 1 to 12. The start of the second iteration is diagrammed as follows:

(13)  $(F_0, F_0', F_0'', F_0''', \bar{F}_1''', \bar{F}_2''', \bar{F}_3''', \bar{F}_4''') \rightarrow \bar{F}_1, \bar{F}_1', \bar{F}_1''$

(14)  $(H_0, H_0', H_0'', \bar{H}_1'', \bar{H}_2'', \bar{H}_3'', \bar{H}_4'') \rightarrow \bar{H}_1, \bar{H}_1'$

(15)  $(\bar{F}_1, \bar{F}_1', \bar{F}_1'', \bar{H}_1, \bar{H}_1') \rightarrow \bar{F}_1''', \bar{H}_1''$

(16)  $(F_0, F_0', F_0'', F_0''', \bar{F}_1''', \bar{F}_2''', \bar{F}_3''', \bar{F}_4''') \rightarrow \bar{F}_2, \bar{F}_2', \bar{F}_2''$

Successive sets of 12 steps are performed until the values of  $F_1'''$  and  $H_1''$  no longer change.

On the IBM Card-Programmed Electronic Calculator, a deck of punched cards 2 inches thick sufficed to perform steps 1 to 12. Three runs of this starter deck at 3 minutes per run accomplished complete convergence in most cases. At the end of the starting process there have been computed and stored  $F_4, F_4', F_4'', H_4$ , and  $H_4'$ , and final estimates of  $F_1'''$ ,  $F_2'''$ ,  $F_3'''$ ,  $F_4'''$ ,  $H_1''$ ,  $H_2''$ ,  $H_3''$ , and  $H_4''$ .

The extension phase has now been reached. It used a different set of integration formulas based on the same general ideas as equations (B3) to (B7). If  $F_0'''$ ,  $F_1'''$ ,  $F_2'''$ ,  $F_3'''$ , and  $F_4'''$  now designate  $F'''$  at any five successive points, and the subscript 5 denotes the next point,

$$F_5'' = F_4'' + \frac{\kappa}{C^{(3)}} \sum_{j=0}^4 B_j^{(3)} F_j''' \quad (B8)$$

$$H_5' = H_4' + \frac{\kappa}{C^{(3)}} \sum_{j=0}^4 B_j^{(3)} H_j'' \quad (B9)$$

$$F_5' = F_4' + \kappa F_4'' + \frac{\kappa^2}{C^{(3)}} \sum_{j=0}^4 B_j^{(3)} F_j''' \quad (B10)$$

$$H_5 = H_4 + \kappa H_4' + \frac{\kappa^2}{C^{(3)}} \sum_{j=0}^4 B_j^{(3)} H_j'' \quad (B11)$$

$$F_5 = F_4 + \kappa F_4' + \frac{\kappa^2}{2} F_4'' + \frac{\kappa^3}{C^{(3)}} \sum_{j=0}^4 B_j^{(3)} F_j''' \quad (B12)$$

where the  $B_j^{(n)}$  and  $C^{(n)}$  are given in the following table:

		$B_j^{(n)}$					$C^{(n)}$
$n \setminus j$	0	1	2	3	4		
1	251	-1274	2016	-2774	1901	720	
2	135	-692	1446	-1596	1427	1440	
3	410	-2116	4476	-5084	5674	20160	

The extension phase may then be diagrammed simply as follows:

- (1)  $(F_4, F_4', F_4'', F_0''', F_1''', F_2''', F_3''', F_4''') \rightarrow F_5, F_5', F_5''$
- (2)  $(H_4, H_4', H_0'', H_1'', H_2'', H_3'', H_4'') \rightarrow H_5, H_5'$
- (3)  $(F_5, F_5', F_5'', H_5, H_5') \rightarrow F_5''', H_5'''$

The values of the functions at the next point are computed in similar manner, where the latest sets of five values of  $F'''$  and  $H''$  are used. This process advances step by step toward infinity.

The extended deck of punched cards was about 3 inches thick and took a little over 3 minutes per run. For  $Pr=0.72$ , a step size of 0.1 was used, the starting phase took 10 minutes, and the extension phase, about 30 minutes. When it is realized that about 11,000 operations were performed in the 40 minutes per run, it may be seen that solution of the present problem would have been prohibitively difficult on desk-type calculators. Simplifications in method would have sacrificed accuracy or required smaller step size.

In two-point boundary-value problems where one point is infinity, some problems of judgment are involved as to where infinity is, and as to when a satisfactory approximation to a solution has been obtained. In most cases this question was settled for the present problem by calling a run satisfactory when it fell between two runs for which  $F'$  and  $H$  did not differ at important points in the fourth decimal place, and

for which  $F'$  and  $H$  flattened out at zero, correct to four decimal places.

Certain difficulties were met in the attempt to use the basic procedure previously discussed. These necessitated certain modifications.

For  $Pr=2, 10, 100$ , and  $1000$ ,  $H$  would settle down to zero at an early stage; but while  $F'$  was still coming down,  $H''$  would begin to oscillate and these oscillations increased and fed back into all other functions. This trouble was avoided by the following modifications: It is a consequence of equation (B2) that

$$H'(\eta) = H'(0) \exp\left(-3Pr \int_0^\eta F(t) dt\right) \\ = H'(\eta - \kappa) \exp\left(-3Pr \int_{\eta-\kappa}^\eta F(t) dt\right) \quad (B13)$$

The extension phase was modified to require the additional integration formulas

$$\int_{\eta-\kappa}^\eta F(t) dt = \frac{\kappa}{720} \sum_{i=1}^5 A_i F_i \quad (B14)$$

$$H_5 = H_4 + \frac{\kappa}{720} \sum_{i=1}^5 A_i H_i' \quad (B15)$$

where  $A_1=-19, A_2=106, A_3=-264, A_4=646$ , and  $A_5=251$ .

These formulas were used along with equations (B8) to (B10) according to the following diagram:

- (1)  $(F_4, F_4', F_4'', F_0''', F_1''', F_2''', F_3''', F_4''') \rightarrow F_5, F_5', F_5''$
- (2)  $(F_1, F_2, F_3, F_4, F_5, H_4') \rightarrow H'$  by means of (B14) and (B13)
- (3)  $(H_1', H_2', H_3', H_4', H_5', H_4) \rightarrow H_5$  by means of (B15)
- (4)  $(F_5, F_5', F_5'', H_5) \rightarrow F_5'''$

The value  $F_0'''$  is discarded and  $F'''$  at the last five points is used to repeat the whole process again and again ad infinitum. As long as  $F$  stays positive,  $H'$  is guaranteed to approach zero and  $H$  will flatten out to some value and not oscillate.

For  $Pr=0.01, 0.72, 0.733$ , and  $1$ , the  $F'''$  began to oscillate at an advanced point and these oscillations grew and fed into the other functions. For all cases but  $Pr=0.01$ , the oscillations appeared very late, near the end of the run, and a suitable halving of step size when oscillation was detected in the fourth differences of  $F'''$  was sufficient to avoid the difficulty. But for the 0.01 case, oscillations of  $F'''$  appeared early in the run, namely, soon after the peak in  $F$ . These oscillations were found to be step-size connected, so that reduction of the step to 0.02 avoided them. Even then oscillations in  $F'''$  would begin to appear every 25 steps or so, and these were smoothed out regularly by repeated runs of a deck similar to the starter deck. Each run under these conditions took about 16 hours, making this the most difficult case to solve.

## APPENDIX C

## DERIVATION OF FLOW PARAMETER

By definition the shear stress is given by

$$\tau = \mu_0 \left( \frac{\partial U}{\partial Y} \right)_0 \quad (C1)$$

To express  $(\partial U / \partial Y)_0$  in terms of the known function  $F(\eta)$ , use can be made of equations (60) and (62). Then

$$\frac{\partial U}{\partial Y} = (4Gr_x^3)^{\frac{1}{2}} \frac{\nu_\infty}{X^2}$$

Substitution of this expression into equation (C1) yields the flow parameter

$$\frac{\tau}{(4Gr_x^3)^{\frac{1}{2}} (\nu_\infty \mu_0 / X^2)} = F''(0)$$

Note that from the general derivation, the flow parameter contains the viscosity evaluated at two different points. Recall, however, that the analysis has shown that to a first approximation the variation of viscosity with temperature can be neglected. Thus the viscosity can be taken as constant in the entire flow field.

## APPENDIX D

## DERIVATION OF HEAT-TRANSFER PARAMETER

The local Nusselt number is defined as

$$Nu = \frac{hX}{k} = \frac{-X}{(T_0 - T_\infty)} \left( \frac{\partial T}{\partial Y} \right)_0 \quad (D1)$$

To express  $(\partial T / \partial Y)_0$  in terms of the known function  $H(\eta)$ , use is made of equations (61) and (62). Thus

$$\frac{\partial T}{\partial Y} = \frac{(T_0 - T_\infty)}{X} \left( \frac{Gr_x}{4} \right)^{\frac{1}{2}} H'(\eta)$$

Substitution of this expression into equation (D1) yields the heat-transfer parameter

$$\frac{Nu}{(Gr_x/4)^{\frac{1}{2}}} = -H'(0) \quad (D2)$$

The heat-transfer parameter as given by equation (D2) is, as was previously stated, a local parameter. It is often desired to compute the average (over the length  $X$ ) value of this parameter. To this end, the Nusselt number (as given in equation (D1)) must be defined in terms of an average heat-transfer coefficient and the quantity thus obtained must then be integrated over the length  $X$  and divided by  $X$ . This procedure yields the result

$$Nu = \frac{3}{4} (Nu)_{av}$$

It is from this last equation that the 0.75 reduction factor previously discussed was obtained.

## REFERENCES

1. Eckert, E. R. G., and Soehngen, E. E.: Studies on Heat Transfer in Laminar Free Convection with the Zehnder-Mach Interferometer. Tech. Rep. No. 5747, A. T. I. No. 44580, Air Materiel Command (Dayton, Ohio), Dec. 27, 1948.
2. Schmidt, Ernst, und Beckmann, Wilhelm: Das Temperatur- und Geschwindigkeitsfeld vor einer Wärme abgebenden senkrechter Platte bei natürlicher Konvektion. Tech. Mech. u. Thermodynamik, Bd. 1, Nr. 10, Okt. 1930, pp. 341-349; cont., Bd. 1, Nr. 11, Nov. 1930, pp. 391-406.
3. Schuh, H.: Boundary Layers of Temperature. Repts. & Trans. 1007, AVA Monographs, British M. A. P., April 15, 1948.
4. Ostrach, Simon: A Boundary Layer Problem in the Theory of Free Convection. Doctoral Thesis, Brown Univ., Aug. 1950.
5. Lewis, J. A.: Boundary Layer in Compressible Fluid. Monograph V, Tech. Rep. No. F-TR-1179-ND (GDAM A-9-M V), Air Materiel Command (Dayton, Ohio), Feb. 1948. (Analysis Div., Intelligence Dept. Contract W33-038-ac-15004 (16351) with Brown Univ.)
6. Zemansky, Mark W.: Heat and Thermodynamics. Second ed., McGraw-Hill Book Co., Inc., 1943, pp. 26-27.
7. Eckert, E. R. G.: Introduction to the Transfer of Heat and Mass. McGraw-Hill Book Co., Inc., 1950.
8. Lagerstrom, Paco, Cole, Julian D., and Trilling, Leon: Problems in the Theory of Viscous Compressible Fluids. Guggenheim Aero. Lab., C. I. T., March 1949, pp. 38-40. (Office of Naval Res. Contract N6onr-Task VIII.)
9. Friedrichs, K. O., and Wasow, W. R.: Singular Perturbations of Non-Linear Oscillations. Duke Math. Jour., vol. 13, 1946, pp. 367-381.
10. Eckert, E. R. G., and Jackson, Thomas W.: Analysis of Turbulent Free-Convection Boundary Layer on Flat Plate. NACA Rep. 1015, 1951. (Supersedes NACA TN 2207.)
11. McAdams, William H.: Heat Transmission. Second ed., McGraw-Hill Book Co., Inc., 1942, p. 242.
12. Lorenz, Hans H.: Die Wärmeübertragung von einer ebenen, senkrechten Platte an Öl bei natürlicher Konvektion. Zs. f. tech. Phys., Nr. 9, Heft 15, 1934, pp. 362-366.
13. Saunders, O. A.: Natural convection in liquids. Proc. Roy Soc. (London), ser. A, vol. 172, no. 948, July 19, 1939, pp. 55-71.







TABLE I.—FUNCTIONS  $F$  AND  $H$  AND DERIVATIVES FOR VARIOUS PRANDTL NUMBERS—Concluded

(g) Prandtl number, 100—Concluded

$\eta$	$F$	$F'$	$F''$	$H$	$H'$
3.2	0.0917	0.0166	-0.0086	0.0000	0.0000
3.4	.0979	.0164	-.0081	.0000	.0000
3.6	.1008	.0142	-.0058	.0000	.0000
3.8	.1035	.0131	-.0052	.0000	.0000
4.0	.1061	.0121	-.0049	.0000	.0000
4.4	.1105	.0103	-.0042	.0000	.0000
4.8	.1143	.0088	-.0036	.0000	.0000
5.2	.1176	.0074	-.0031	.0000	.0000
5.6	.1203	.0063	-.0026	.0000	.0000
6.0	.1226	.0053	-.0022	.0000	.0000
6.6	.1254	.0041	-.0018	.0000	.0000
7.2	.1276	.0032	-.0014	.0000	.0000
8.0	.1297	.0022	-.0010	.0000	.0000
9.0	.1315	.0014	-.0007	.0000	.0000
10.0	.1326	.0008	-.0005	.0000	.0000
11.0	.1332	.0004	-.0003	.0000	.0000
12.0	.1335	.0002	-.0002	.0000	.0000
13.0	.1338	.0000	-.0001	.0000	.0000

(h) Prandtl number, 1000

$\eta$	$F$	$F'$	$F''$	$H$	$H'$
0.	0.0000	0.0000	0.1450	1.0000	-3.966
.025	.0000	.0033	.1212	.9009	-3.962
.050	.0002	.0061	.0999	.8021	-3.933
.075	.0003	.0083	.0811	.7046	-3.881
.100	.0006	.0102	.0647	.6096	-3.731
.125	.0008	.0116	.0506	.5186	-3.538
.150	.0012	.0127	.0387	.4332	-3.283
.175	.0015	.0135	.0289	.3549	-2.975
.200	.0018	.0142	.0209	.2847	-2.628
.225	.0022	.0146	.0140	.2236	-2.261
.250	.0026	.0149	.0086	.1717	-1.893
.275	.0029	.0151	.0059	.1288	-1.541
.300	.0033	.0152	.0032	.0944	-1.220
.325	.0037	.0153	.0012	.0675	-.9331
.350	.0041	.0153	-.0003	.0471	-.7012
.375	.0045	.0152	-.0012	.0321	-.5033
.400	.0048	.0152	-.0019	.0213	-.3596
.425	.0052	.0152	-.0023	.0138	-.2467
.450	.0056	.0151	-.0026	.0087	-.1645
.475	.0060	.0150	-.0027	.0053	-.1066
.500	.0063	.0150	-.0028	.0032	-.0672
.525	.0067	.0149	-.0029	.0019	-.0413
.550	.0071	.0148	-.0029	.0011	-.0245
.575	.0075	.0147	-.0029	.0006	-.0142
.600	.0078	.0147	-.0029	.0003	-.0080
.625	.0082	.0146	-.0029	.0002	-.0044
.800	.0107	.0141	-.0028	.0000	.0000
1.000	.0135	.0136	-.0027	.0000	.0000
1.40	.0187	.0125	-.0025	.0000	.0000
1.80	.0235	.0115	-.0023	.0000	.0000
2.20	.0279	.0106	-.0022	.0000	.0000
2.60	.0320	.0098	-.0020	.0000	.0000
3.0	.0358	.0090	-.0019	.0000	.0000
3.6	.0409	.0080	-.0017	.0000	.0000
4.2	.0464	.0070	-.0015	.0000	.0000
5.0	.0505	.0060	-.0012	.0000	.0000
5.8	.0549	.0050	-.0011	.0000	.0000
7.0	.0603	.0039	-.0008	.0000	.0000
8.0	.0638	.0032	-.0007	.0000	.0000
10.0	.0691	.0022	-.0004	.0000	.0000
12.0	.0727	.0015	-.0003	.0000	.0000
14.0	.0752	.0011	-.0002	.0000	.0000
16.0	.0771	.0008	-.0001	.0000	.0000
18.0	.0786	.0007	.0000	.0000	.0000
20.0	.0798	.0006	.0000	.0000	.0000
22.0	.0809	.0005	.0000	.0000	.0000
23.6	.0816	.0005	.0000	.0000	.0000

